

0622

Frequency Drift in MR Spectroscopy: An 87-scanner 3T Phantom Study

Steve C.N. Hui^{1,2}, Mark Mikkelsen^{1,2}, Helge J. Zöllner^{1,2}, Vishwadeep Ahluwalia³, Sarael Alcauter⁴, Laima Baltusis⁵, Deborah A. Barany⁶, Laura R. Barlow⁷, Robert Becker⁸, Jeffrey I. Berman⁹, Adam Berrington¹⁰, Pallab K. Bhattacharyya¹¹, Jakob Udby Blicher¹², Wolfgang Bogner¹³, Mark S. Brown¹⁴, Vince D. Calhoun¹⁵, Ryan Castillo¹⁶, Kim M. Cecil¹⁷, Yeo Bi Choi¹⁸, Winnie C.W. Chu¹⁹, William T. Clarke²⁰, Alexander R. Craven²¹, Koen Cuyppers²², Michael Dacko²³, Camilo de la Fuente-Sandoval²⁴, Patricia Desmond²⁵, Aleksandra Domagalik²⁶, Julien Dumont²⁷, Niall W. Duncan²⁸, Ulrike Dydak²⁹, Katherine Dyke³⁰, David A. Edmondson³¹, Gabriele Ende³², Lars Erslund³³, C. John Evans³⁴, Alan S. R. Fermis³⁵, Antonio Ferretti³⁴, Ariane Fillmer³⁵, Tao Gong³⁶, Ian Greenhouse³⁷, James T. Grist³⁸, Meng Gu³⁹, Ashley D. Harris⁴⁰, Katarzyna Ha⁴¹, Stefanie Heba⁴², Eva Heckova⁴³, John P. Hegarty II⁴³, Kirstin-Friederike Heise⁴⁴, Aaron Jacobson⁴⁵, Jacobus F.A. Jansen⁴⁶, Christopher W. Jenkins⁴⁷, Stephen J. Johnston⁴⁸, Christoph Juchem⁴⁹, Alayar Kangarlu⁵⁰, Adam B. Kerr⁵¹, Karl Landheer⁵¹, Thomas Lange⁵², Phil Lee⁵³, Swati Rane Levendovszky⁵⁴, Catherine Limperopoulos⁵⁵, Feng Liu⁵⁶, William Lloyd⁵⁷, David J. Lythgoe⁵⁸, Maro G. Machizawa⁵⁹, Erin L. MacMillan⁶⁰, Richard J. Maddock⁶⁰, Andrei V. Manzhurteev⁶¹, Maria L. Martinez-Gudino⁶², Jack J. Miller⁶³, Heline Mirzakhania⁶⁴, Paul G. Mullins⁶⁵, Jamie Near⁶⁶, Wibeke Nordhøy⁶⁷, Georg Oeltzschner^{1,2}, Raul Osorio⁶⁸, Maria C.G. Otaduy⁶⁸, Erick H. Pasaye⁶⁹, Ronald Peeters⁶⁹, Scott J. Peltier⁷⁰, Ulrich Pilatus⁷¹, Nenad Polomac⁷¹, Eric C. Porges⁷², Subechhya Pradhan⁷³, James Puts⁷⁴, Caroline D. Rae⁷⁵, Francisco Reyes-Madriral⁷⁶, Timothy P.L. Roberts⁷⁷, Caroline E. Robertson⁷⁷, Muhammad G. Saleh⁷⁸, Jens T. Rosenberg⁷⁹, Diana-Georgiana Rotaru⁵⁸, O'Gorman Tuura L. Ruth⁸⁰, Kristian Sandberg¹², Ryan Sangill⁸¹, Keith Schembri⁸², Anouk Schreanet⁸³, Natalia A. Semenova⁸⁴, Debra Singe⁸⁵, Rouslan Sitnikov⁸⁶, Jolinda Smith⁸⁷, Yulu Song³⁶, Craig Stark⁸⁸, Diederick Stoffers⁸⁹, Stephan P. Swinnen⁴⁴, Costin Tanase⁶⁰, Sofie Tapper^{1,2}, Martin Tegenthoff⁴², Thomas Thiel⁹⁰, Marc Thioux⁹¹, Peter Truong⁹², Pim van Dijk⁹³, Nolan Vella⁹², Rishma Vidyasagar⁹³, Andrej Vovk⁹⁴, Guangbin Wang³⁶, Lars T. Westle⁶⁷, Timothy K. Wilbur⁵⁴, William R. Willoughby⁹⁵, Martin Wilson⁹⁶, Hans-Jörg Wittsack⁹⁷, Adam J. Woods⁹⁸, Yen-Chien Wu⁹⁹, Junqian Xu¹⁰⁰, Maria Yanez Lopez¹⁰¹, David K.W. Yeung⁹⁹, Qun Zhao¹⁰², Xiaopeng Zhou⁹⁹, Gasper Zupan⁹⁴, and Richard A.E. Edden^{1,2}

¹Russell H. Morgan Department of Radiology and Radiological Science, The Johns Hopkins University School of Medicine, Baltimore, MD, United States, ²F.M. Kirby Research Center for Functional Brain Imaging, Kennedy Krieger Institute, Baltimore, MD, United States, ³GSU/GT Center for Advanced Brain Imaging, Georgia Institute of Technology, Atlanta, GA, United States, ⁴Instituto de Neurobiología, Universidad Nacional Autónoma de México, Queretaro, Mexico, ⁵Center for Cognitive and Neurobiological Imaging, Stanford University, Stanford, CA, United States, ⁶Kinesiology, University of Georgia, Athens, GA, United States, ⁷Department of Radiology, The University of British Columbia, Vancouver, BC, Canada, ⁸Center for Innovative Psychiatry and Psychotherapy Research, Department Neuroimaging, Central Institute of Mental Health, Medical Faculty Mannheim, Heidelberg University, Mannheim, Germany, ⁹Department of Radiology, Children's Hospital of Philadelphia, Philadelphia, PA, United States, ¹⁰Sir Peter Mansfield Imaging Centre, School of Physics and Astronomy, University of Nottingham, Nottingham, United Kingdom, ¹¹Imaging Institute, The Cleveland Clinic, Cleveland, OH, United States, ¹²Center of Functionally Integrative Neuroscience, Aarhus University, Aarhus, Denmark, ¹³Department of Biomedical Imaging and Image-guided Therapy, High-Field MR Center, Medical University of Vienna, Vienna, Austria, ¹⁴Department of Radiology, University of Colorado Anschutz Medical Campus, Aurora, CO, United States, ¹⁵Tr-Institutional Center for Translational Research in Neuroimaging and Data Science (TReNDS), Georgia State University, Georgia Institute of Technology, and Emory University, Atlanta, GA, United States, ¹⁶Neuroscience Research Australia/NeuRA Imaging, Randwick, Australia, ¹⁷Department of Radiology, Cincinnati Children's Hospital Medical Center, Cincinnati, OH, United States, ¹⁸Psychological and Brain Sciences, Dartmouth College, Hanover, NH, United States, ¹⁹Department of Imaging & Interventional Radiology, The Chinese University of Hong Kong, Hong Kong, ²⁰Wellcome Centre for Integrative Neuroimaging, NDCN, University of Oxford, Oxford, United Kingdom, ²¹Department of Biological and Medical Psychology, University of Bergen, Haukeland University Hospital, Bergen, Norway, ²²REVAL Rehabilitation Research Institute (REVAL), Hasselt University, Diepenbeek, Belgium, ²³Department of Radiology, Medical Physics, Medical Center - University of Freiburg, Faculty of Medicine, University of Freiburg, Freiburg, Germany, ²⁴Laboratory of Experimental Psychiatry & Neuropsychiatry Department, Instituto Nacional de Neurología y Neurocirugía, Mexico City, Mexico, ²⁵Department of Radiology, University of Melbourne/Royal Melbourne Hospital, Melbourne, Australia, ²⁶Malopolska Centre of Biotechnology, Jagiellonian University, Krakow, Poland, ²⁷Clinical Imaging Core Facility, C12C Lille, Lille, France, ²⁸Graduate Institute of Mind, Brain and Consciousness, Taipei Medical University, Taipei, Taiwan, ²⁹School of Health Sciences, Purdue University, West Lafayette, IN, United States, ³⁰School of Psychology, University of Nottingham, Nottingham, United Kingdom, ³¹Department of Clinical Engineering, University of Bergen, Haukeland University Hospital, Bergen, Norway, ³²CUBRIC, Cardiff University, Cardiff, United Kingdom, ³³Center for Brain, Mind and KANSEI Sciences Research, Hiroshima University, Hiroshima, Japan, ³⁴Neuroscience, Imaging and Clinical Sciences, University "G. d'Annunzio" of Chieti-Pescara, Chieti, Italy, ³⁵Physikalisch-Technische Bundesanstalt (PTB), Braunschweig and Berlin, Germany, ³⁶Department of Imaging and Nuclear Medicine, Shandong Medical Imaging Research Institute, Shandong University, Jinan, China, ³⁷Human Physiology, University of Oregon, Eugene, OR, United States, ³⁸Physiology, Anatomy, and Genetics/ Oxford Centre for Magnetic Resonance, The University of Oxford / Department of Radiology, The Churchill Hospital, The University of Oxford, Oxford, United Kingdom, ³⁹Department of Radiology, Stanford University, Stanford, CA, United States, ⁴⁰Department of Radiology, University of Calgary, Calgary, AB, Canada, ⁴¹Institute of Psychology, Jagiellonian University, Krakow, Poland, ⁴²Department of Neurology, BG University Hospital Bergmannsheil, Bochum, Germany, ⁴³Psychiatry & Behavioral Sciences, Stanford University, Stanford, CA, United States, ⁴⁴Department of Movement Sciences, KU Leuven, Leuven, Belgium, ⁴⁵Department of Radiology, University of California San Diego, San Diego, CA, United States, ⁴⁶Department of Radiology and Nuclear Medicine, Maastricht University Medical Center, Maastricht, Netherlands, ⁴⁷CUBRIC, Cardiff University, Cardiff, United Kingdom, ⁴⁸Psychology Dept. / Clinical Imaging Facility, Swansea University, Swansea, United Kingdom, ⁴⁹Biomedical Engineering and Radiology, Columbia University, New York City, NY, United States, ⁵⁰Psychiatry, Columbia University Irving Medical Center/New York State Psychiatric Institute, New York City, NY, United States, ⁵¹Biomedical Engineering, Columbia University, New York City, NY, United States, ⁵²Department of Radiology, Medical Physics, University of Freiburg, Freiburg, Germany, ⁵³Department of Radiology, University of Kansas Medical Center, Kansas, KS, United States, ⁵⁴Department of Radiology, University of Washington, Seattle, WA, United States, ⁵⁵Developing Brain Institute, Diagnostic Imaging and Radiology, Children's National Hospital, Washington, DC, United States, ⁵⁶Department of Psychiatry, Columbia University Irving Medical Center/New York State Psychiatric Institute, New York, NY, United States, ⁵⁷Division of Informatics, Imaging & Data Sciences, University of Manchester, Manchester, United Kingdom, ⁵⁸Department of Neuroimaging, King's College London, London, United Kingdom, ⁵⁹Center for Brain, Mind and KANSEI Sciences Research, Hiroshima University, Hiroshima, Japan, ⁶⁰Psychiatry and Behavioral Sciences, University of California Davis, Imaging Research Center, Davis, CA, United States, ⁶¹Department of Radiology, Clinical and Research Institute of Emergency Pediatric Surgery and Trauma, Moscow, Russian Federation, ⁶²Imágenes Cerebrales, Instituto Nacional de Psiquiatría Ramón de la Fuente, Mexico City, Mexico, ⁶³Department of Physics, University of Oxford, Oxford, United Kingdom, ⁶⁴Department of Psychiatry, University of California San Diego, San Diego, CA, United States, ⁶⁵Department of Psychology, Bangor University, Bangor, United Kingdom, ⁶⁶Douglas Mental Health University Institute and Department of Psychiatry, McGill University, Montreal, QC, Canada, ⁶⁷Department of Diagnostic Physics, Division of Radiology and Nuclear Medicine, Oslo University Hospital, Oslo, Norway, ⁶⁸LIM44, Instituto e Departamento de Radiologia, Faculdade de Medicina, Universidade de Sao Paulo, Sao Paulo, Brazil, ⁶⁹Department of Imaging & Pathology, Department of Radiology, University Hospitals Leuven, KU Leuven, Leuven, Belgium, ⁷⁰Functional MRI Laboratory, University of Michigan, Ann Arbor, MI, United States, ⁷¹Institute of Neuroradiology, Goethe-University Frankfurt, Frankfurt, Germany, ⁷²Center for Cognitive Aging and Memory, McKnight Brain Institute, Department of Clinical and Health Psychology, College of Public Health and Health Professions, University of Florida, Gainesville, FL, United States, ⁷³Psychiatry and Behavioral Sciences, Medical University of South Carolina, Charleston, SC, United States, ⁷⁴Forensic & Neurodevelopmental Sciences, King's College London, London, United Kingdom, ⁷⁵NeuRA Imaging, Neuroscience Research Australia, Randwick, Australia, ⁷⁶Laboratory of Experimental Psychiatry, Instituto Nacional de Neurología y Neurocirugía, Mexico City, Mexico, ⁷⁷Department of Psychological and Brain Sciences, Dartmouth College, Hanover, NH, United States, ⁷⁸Department of Diagnostic Radiology and Nuclear Medicine, University of Maryland School of Medicine, Baltimore, MD, United States, ⁷⁹McKnight Brain Institute, AMRIS, University of Florida, Gainesville, FL, United States, ⁸⁰Center for MR Research, University Children's Hospital, Zurich, Switzerland, ⁸¹Center of Functionally Integrative Neuroscience, Aarhus University Hospital, Aarhus, Denmark, ⁸²Medical Physics, Mater Dei Hospital, Msida, Malta, ⁸³Department of Radiology and Nuclear Medicine, Amsterdam University Medical Center, University of Amsterdam, Amsterdam, Netherlands, ⁸⁴S04, Emanuel Institute of Biochemical Physics of the Russian Academy of Sciences, Moscow, Russian Federation, ⁸⁵Psychiatry, University of Colorado Anschutz Medical Campus, Aurora, CO, United States, ⁸⁶Clinical Neuroscience, MRI Center, Karolinska Institutet, Clinical Neuroscience, MRI Center, Sweden, ⁸⁷Lewis Center for Neuroimaging, University of Oregon, Eugene, OR, United States, ⁸⁸Department of Neurobiology and Behavior, Facility for Imaging and Brain Research (FIBRE) & Campus Center for Neuroimaging (CCNI), University of California, Irvine, Irvine, CA, United States, ⁸⁹Spinoza Centre for Neuroimaging, Royal Netherlands Academy of Arts and Sciences, Amsterdam, Netherlands, ⁹⁰Institute of Clinical Neuroscience and Medical Psychology, University Dusseldorf, Medical Faculty, Dusseldorf, Germany, ⁹¹Otorhinolaryngology, Head and Neck Surgery, University of Groningen, University Medical Center Groningen, Groningen, Netherlands, ⁹²Brain Health Imaging Centre, Centre for Addiction and Mental Health, Toronto, ON, Canada, ⁹³Melbourne Dementia Research Centre, Florey Institute of Neurosciences and Mental Health, Melbourne, Australia, ⁹⁴Faculty of Medicine, University of Ljubljana, Ljubljana, Slovenia, ⁹⁵Department of Radiology, University of Alabama at Birmingham, Birmingham, AL, United States, ⁹⁶Centre for Human Brain Health, University of Birmingham, Birmingham, United Kingdom, ⁹⁷Department of Diagnostic and Interventional Radiology, University Dusseldorf, Medical Faculty, Dusseldorf, Germany, ⁹⁸Center for Cognitive Aging and Memory, McKnight Brain Institute, Department of Clinical and Health Psychology, College of Public Health and Health Professions, Department of Neuroscience, College of Medicine, University of Florida, Gainesville, FL, United States, ⁹⁹Department of Radiology, TMU-Shuang Ho Hospital, New Taipei City, Taiwan, ¹⁰⁰Department of Radiology and Psychiatry, Baylor College of Medicine, Houston, TX, United States, ¹⁰¹Perinatal Imaging & Health, King's College London, London, United Kingdom, ¹⁰²Biomedical Research Center, University of Georgia, Athens, GA, United States

Synopsis

This project aimed to examine the relationship between gradient-induced heating and field drift on a large sample of MRI scanners. A standardized phantom protocol was established, and spectroscopy was performed before and after running 10 minutes of echo-planar imaging (EPI). MRS data were acquired from 87 scanners. The frequency drift trace was extracted by modeling the water signal in each transient. Drift rates of up to 1.3 Hz/minute were seen before EPI, and 4 Hz/minute after. This dataset will allow sites to benchmark scanner drift, for consideration in planning research protocol order and examine the need for real-time field-frequency locking.

Introduction

Heating of the gradient coils and thermal dissipation to the passive shims is a common cause of instability in the B₀ field, especially when echo-planar imaging (EPI) sequences are used (1-3). B₀ field drift changes the resonance frequency of spins, resulting in line broadening, decreased SNR and changes in editing efficiency for edited MRS experiments which rely on accurately placing frequency-selective pulses. To examine the extent and impact of gradient-induced frequency drift, a standardized protocol was distributed to sites with scanners from three vendors. By collecting data from a large number of sites, we aim to establish 'typical' levels of drift for benchmarking purposes, and to assess whether there is a widespread need for real-time field-frequency locking (2).

Methods

Phantom water signals were acquired with PRESS localization before and after a BOLD-weighted fMRI sequence. Standardized protocols were generated for GE, Philips and Siemens scanners consisting of: minimal preparatory imaging; pre-fMRI PRESS (TR/TE 5000/35 ms; 64 transients with data stored separately; no water suppression; voxel size 2 × 2 × 2 cm³, duration = 5:20 min); EPI BOLD sequence based on the ADNI-3 (4) protocol (TR/TE 3000/30 ms; 197 dynamics of one average; EPI factor 31, scan duration 10 min); and a long post-fMRI PRESS sequence (360 transients; and same parameters as pre-fMRI PRESS). Sites were instructed to use a water-dominant phantom of spherical or cylindrical shape. Phased-array head or head-and-neck coils with between 8 and 64 channels were used. Scanning was performed at least 6 hours after the previous scan to avoid any drift confounds due to heating effects. Phantoms were acclimatized in the scan room for the same period, and positioned at scanner isocenter. Spectral analysis was performed using MATLAB (R2020b, MathWorks, Natick, USA), including eddy-current correction, zero-filling and Fourier transformation. Frequency-domain pre- and post-fMRI PRESS spectra were modeled using a Lorentzian-Gaussian (Voigt) lineshape model to extract the water peak center frequency from each individual transient. In order to compare frequency drift before and after EPI, the mean absolute frequency offset of the first 64 dynamics was calculated, and paired t-test was performed between pre- and post-fMRI PRESS. To visualize the effect of the observed frequency drifts on a typical 5-minute in vivo protocol, a simulated in vivo spectrum was generated using FID-A (5), including 18 major metabolites (TE = 35 ms; 2048 samples; 2 kHz spectral width, 2 Hz linewidth). The simulated spectrum was convolved with the frequency trace from the first 64 TRs of the phantom recording and spectra plotted. Fifty-eight sites repeated the acquisition protocol on a different day to allow investigation of the reproducibility of frequency drift traces. Pearson and intraclass correlation coefficients (ICC) were calculated between the two runs using the 'psych' R package (6). ICC calculation was based on a two-way mixed-effects model with average measures of absolute agreement.

Results

Data were received from 71 sites and 87 scanners (GE = 20, Philips = 28, Siemens = 39; 58 scanners submitted repeat data). Figure 1 shows the individual spectra for the highest-drifting scanner, before and after fMRI, with the frequency drift traces. Figure 2 shows the frequency drift traces overlaid for all 87 scanners. Scanners drifted by up to 7 Hz within 5 minutes before fMRI and by up to 26 Hz within 30 minutes after fMRI. Figure 3 shows a box plot of the absolute average frequency offset of each scanner (7). The mean absolute frequency offset across 64 transients (~5 min) was 0.78 ± 0.87 Hz (median = 0.4 Hz) and 1.33 ± 1.42 Hz (median = 0.8 Hz) respectively before and after fMRI. T-tests indicated drifting was significantly increased ($p < 0.05$) after fMRI, as expected. Simulated spectra that have been convolved with 64-transient water traces (the highest and lowest drift case for each vendor pre- and post-fMRI) are shown in Figure 4. The intensity of the NAA singlet is reduced by up to 26%, 44 % and 18% for GE, Philips and Siemens respectively, after fMRI. Since drift does not impact the noise, these peak signal losses represent predicted losses of SNR. Drift behavior was well correlated and reproducible. ICCs were 0.85 and 0.95 for pre- and post-fMRI PRESS repeated datasets, respectively. Pearson correlation coefficients (0.74 and 0.90) also showed good correlation between repeated datasets.

Discussion

Frequency drift data are presented for eighty-seven 3T MRI scanners. Median levels of drift were relatively low (5-minute average under 1 Hz), but the most extreme case suffered from higher levels of drift (up to 3.5 Hz before and 7.2 Hz after fMRI). These levels of drift lead to a measurable loss in SNR for short-TE MRS, as well as changes in editing efficiency and subtraction artefacts in edited MRS. Although the difference between pre- and post-fMRI was significant, it was lower than expected and there appears to be substantial drift associated with running scans 'from cold', as indicated by the pre-fMRI traces after only minimal preparatory imaging. Correlation analysis indicated that the drift was highly repeatable between sessions, so one might expect drift associated with previous scans within a protocol to be consistent.

Acknowledgements

This work was supported by NIH grants R01 EB016089, R01 EB023963, R21 AG060245, K99 EB028828 and K99 AG062230.

References

1. Foerster BU, Tomasi D, Caparelli EC. Magnetic field shift due to mechanical vibration in functional magnetic resonance imaging. *Magn Reson Med* 2005;54(5):1261-1267.
2. Henry PG, van de Moortele PF, Giacomini E, Nauerth A, Bloch G. Field-frequency locked in vivo proton MRS on a whole-body spectrometer. *Magn Reson Med* 1999;42(4):636-642.
3. Rowland BC, Liao H, Adan F, Mariano L, Irvine J, Lin AP. Correcting for Frequency Drift in Clinical Brain MR Spectroscopy. *J Neuroimaging* 2017;27(1):23-28.
4. Weiner MW, Veitch DP, Aisen PS, et al. The Alzheimer's Disease Neuroimaging Initiative 3: Continued innovation for clinical trial improvement. *Alzheimers Dement* 2017;13(5):561-571.
5. Simpson R, Devenyi GA, Jezard P, Hennessy TJ, Near J. Advanced processing and simulation of MRS data using the FID appliance (FID-A)-An open source, MATLAB-based toolkit. *Magn Reson Med* 2017;77(1):23-33.
6. R Core Team R: A Language and Environment for Statistical Computing. R Foundation for Statistical Computing, Vienna, Austria. 2020.
7. Zöllner HJ, Považan M, Hui SCN, Tapper S, Edden RAE, Oeltzschner G. Comparison of different linear-combination modelling algorithms for short-TE proton spectra. *bioRxiv* 2020:2020.2006.2005.136796.

Figures

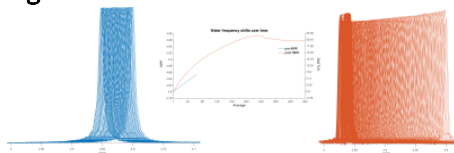


Figure 1. Individual transients of pre- and post-fMRI PRESS (plotted in blue and red, respectively) from the highest-drifting scanner. The frequency offset derived from modeling the water signals is plotted (middle). 360 averages correspond to 30 minutes total scan duration.

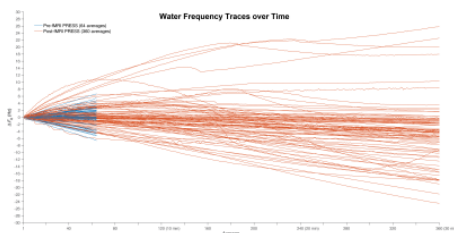


Figure 2. Water offset traces of all 87 scanners. Pre- and post-fMRI traces are plotted in blue and red, respectively. 360 averages correspond to 30 minutes total scan duration.

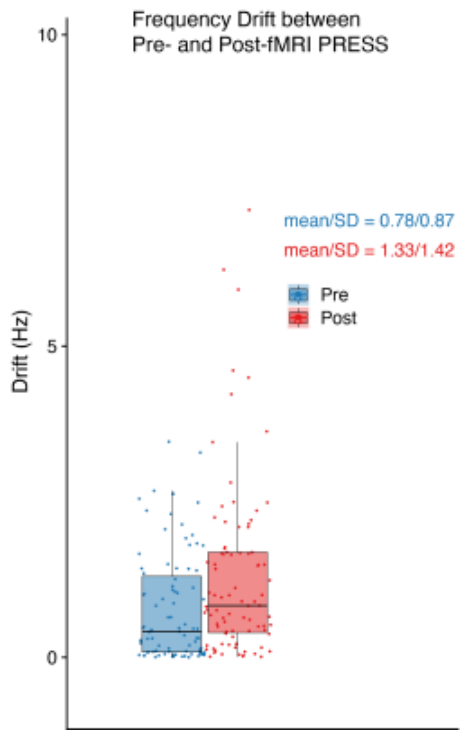


Figure 3. Box plot for the mean absolute frequency offset for pre- and post-fMRI PRESS data on each scanner.

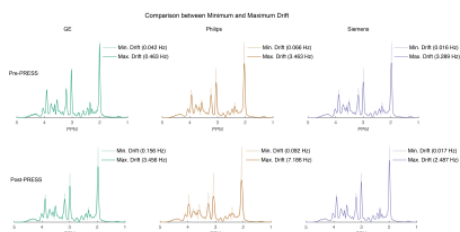


Figure 4. Comparison of simulated spectra with frequency drift applied between minimum and maximum drift for pre- and post-fMRI PRESS data. The minimum-drift case for each vendor (50% opacity) is overlaid with the maximum-drift case (opaque).